

# Extended X-ray absorption fine structure spectroscopic analysis of cation local environment in model polyurethane ionomers

Susan A. Visser and Stuart L. Cooper\*

Department of Chemical Engineering, University of Wisconsin-Madison, Madison, WI 53706, USA

(Received 26 September 1990; revised 16 January 1991; accepted 22 January 1991)

The local environment of the neutralizing cation was examined by extended X-ray absorption fine structure spectroscopy in a series of model polyurethane ionomers. Polyol type, polyol molecular weight and pendant anion type had small effects on cation local environment. Sample preparation conditions had a noticeable effect in one case. The type of cation was the dominant factor in determining local ordering. The degree of local order decreased with cation type in the order  $\text{Ni}^{2+} > \text{Sr}^{2+} > \text{Cd}^{2+}$ , in agreement with the trend of decreasing tensile properties with cation type. Hydration of  $\text{Ni}^{2+}$ -neutralized ionomers induced no change in the  $\text{Ni}^{2+}$  local environment for a sulphonated ionomer, but hydration caused a rapid change in the local structure of the analogous carboxylated ionomer. The changes were in accord with water molecules coordinating to the  $\text{Ni}^{2+}$  cation.

(Keywords: ionomer; polyurethane ionomer; extended X-ray absorption fine structure spectroscopy; local structure; chemical architecture)

## INTRODUCTION

In the previous study<sup>1</sup> on the effect of neutralizing cation on the morphology and properties of model polyurethane ionomers, the contents and arrangement of the elements of the ionic aggregates were shown to influence greatly the physical properties of the ionomers. Small-angle X-ray scattering (SAXS) results indicated that ionic packing arrangements differed in sulphonated and carboxylated ionomers; the differences in anion distribution were correlated with the inflection modulus values obtained from dynamic mechanical analysis. The tensile properties of the ionomers were strongly influenced by cation type, and it was postulated that the local environment of the cation was a dominant influence in the ionomer tensile properties.

The correspondence of ionomer tensile properties and cation local ordering has been observed previously<sup>2-5</sup>. In carboxytelechelic polyisoprene ionomers, it was found that strain-hardening behaviour observed in  $\text{Ni}^{2+}$ - and  $\text{Ca}^{2+}$ -neutralized ionomers could be explained by the presence of a second coordination shell around the neutralizing cation<sup>2</sup>. It was suggested that the higher degree of order in these ionomers resulted in more cohesive ionic aggregates, the physical crosslinks of ionomers, so that stressed chains could not relax by ion hopping. (Ion hopping is the redistribution of ionic groups between aggregates<sup>6-8</sup>.) Thus, the materials with tightly bound aggregates exhibited strain hardening and subsequent sample failure. A similar explanation was

advanced for the correlation observed between cation local structure and tensile properties in sulphonated polyurethane ionomers based on poly(tetramethylene oxide) of molecular weight 1000 (PTMO(1000)) and toluene diisocyanate (TDI)<sup>3-5</sup>. The question of whether this correspondence will continue in other ionomer systems remains open.

The small size and imperfect packing of the ionic aggregates preclude the use of diffraction techniques to determine the local structure in ionomers. In contrast, extended X-ray absorption fine structure spectroscopy (e.x.a.f.s.) can be used to elucidate the local environment of a specific atom and has been applied in a number of ionomer systems<sup>2,5,9-17</sup>. The technique utilizes the modulation of the X-ray absorption coefficient on the high-energy side of an elemental absorption edge to extract information on the number and type of atoms surrounding the atom of interest (the cation in ionomers) and on the size of the coordination shells and their disorder in the bulk. Using e.x.a.f.s., local structures have been shown to vary with cation type<sup>2,5,9,18</sup>, pendant anion type<sup>9</sup>, ionic content<sup>10</sup>, neutralization conditions<sup>13,14</sup>, hydration<sup>15,16,18</sup> and sample treatment<sup>11,17</sup>. Because of the number of factors involved, further studies of the cation local environment in well defined ionomer systems are vital.

In this paper, the local environment of the neutralizing cation is examined in a series of model polyurethane ionomers neutralized with  $\text{Ni}^{2+}$ ,  $\text{Sr}^{2+}$ , or  $\text{Cd}^{2+}$ . The effect of polyol type, ionic group content, pendant anion type, overneutralization, sample preparation conditions and hydration are examined.

\* To whom correspondence should be addressed

## EXPERIMENTAL

*Sample preparation and e.x.a.f.s. measurements*

The synthesis of the polyurethane ionomers was described previously<sup>1,19</sup>. The model polyurethane ionomers are 1:1 copolymers of a polyol and toluene diisocyanate (TDI), which have propyl sulphonate or ethyl carboxylate groups grafted solely at the urethane linkages. Three polyol types were investigated: poly(tetramethylene oxide) (PTMO,  $M_n = 990, 2070$ ), poly(propylene oxide) (PPO, average molecular weight 1000, 2000) and poly(ethylene oxide) (PEO, average molecular weight 1000). Ionomers neutralized with  $Ni^{2+}$ ,  $Sr^{2+}$  and  $Cd^{2+}$  were obtained as previously described<sup>1,3</sup>.

Sample preparation conditions are labelled as either 'solvent-cast' or 'compression-moulded'. The solvent-cast sulphonated ionomers were cast at 60°C from *N,N'*-dimethylacetamide. The solvent-cast carboxylated ionomers were cast at 25°C from 4:1 v/v toluene/methanol, except for the carboxylated PTMO(1000)/TDI ionomers because of solubility constraints. (The parenthetical '1000' indicates the approximate molecular weight of the PTMO polyol.) The carboxylated PTMO(1000)/TDI ionomers were cast from 2:1 v/v toluene/methanol solutions. Compression-moulded samples were moulded at 160°C for 5 min at 10 kpsi ( $\sim 6.9$  MPa). Samples were dried in a 50°C vacuum oven for at least one week prior to testing to remove residual solvent and water. Complete removal of residual polar solvents is difficult for ionomers, as the polar solvent molecules have a tendency to complex with the ionic groups. Thus, while these polymers are as dry as possible, they may not display the morphology and properties of a completely dry ionomer. As this is a problem characteristic of all ionomers, however, the results of this paper are expected to be comparable to data presented for any 'dry' ionomer.

For the e.x.a.f.s. measurements, solvent-cast films were stacked to obtain sufficient absorbance for a good signal-to-noise ratio; compression-moulded samples were moulded to appropriate thicknesses. Hydration of the compression-moulded M2S*Ni* and M2C*Ni* (see next section for notation) samples was achieved by immersion of the samples into distilled water at room temperature for the specified hydration time. Samples were enclosed in a sealed Kapton box during the e.x.a.f.s. measurements in order to prevent sample drying.

The transmission e.x.a.f.s. spectra were collected at the Cornell High Energy Synchrotron Source (CHESS). The samples were studied at the C-2 station. All samples were studied at the K edges of the cations. Data reduction followed a standard procedure of pre-edge and post-edge background removal, extraction of the e.x.a.f.s. oscillations  $\chi(k)$ , Fourier transformation of  $\chi(k)$  and final application of an inverse transform to isolate the e.x.a.f.s. contribution from a selected region in real space<sup>20-22</sup>. The model compounds used were discussed previously<sup>2</sup>.

*Sample nomenclature*

Sample designations are as in the previous paper<sup>1</sup>: the first letter indicates the soft-segment type (M = PTMO, P = PPO, E = PEO); the number indicates the soft-segment molecular weight in thousands; the next letter describes the pendant ionic-group type (S = sulphonate; C = carboxylate); and the final two letters are the chemical symbol for the neutralizing cation.

## RESULTS AND DISCUSSION

E.x.a.f.s. is uniquely suited to determination of the local environment of the cation in ionomers, providing information on the number and type of atoms surrounding the neutralizing cation to a distance of  $\sim 5$  Å. Its weakness is that it gives an average measure of all cation environments in the sample. It is expected that two environments exist for cations in ionomers, one for the cations in the ionic aggregates and another for those cations dispersed in the polymer matrix. To interpret the data presented here, it was postulated that the coordination environment in the ionic aggregates would be more highly ordered than that of the dispersed cations and that the more ordered environment would provide the dominant contribution to the e.x.a.f.s. signal. For the samples in which the e.x.a.f.s. data indicate a disordered local environment, this assumption was not necessary. The possible implications of the averaging inherent in the e.x.a.f.s. technique should be borne in mind.

The e.x.a.f.s. signal is a modulation of the X-ray absorption coefficient on the high-energy side of an elemental absorption edge. The e.x.a.f.s. signal arises because photoelectrons that are ejected by the absorbed X-rays can be backscattered by atoms coordinated to the absorbing atom. Superposition of the outgoing and backscattered electron waves gives rise to an interference pattern. The e.x.a.f.s. signal,  $\chi(k)$ , where  $k$  is the photoelectron wavevector, contains information on the number,  $N_j$ , and type of atoms in coordination shell  $j$ , the distance,  $R_j$ , to this shell, and the static and vibrational disorder of the shell, embodied in the Debye-Waller factor,  $\sigma_j$ . To convert the e.x.a.f.s. signal from wavevector to real space, it is Fourier transformed; the magnitude of the transform is termed the radial structure function (*RSF*). Each non-artifactual peak in the *RSF* represents a distinct coordination shell. (Artifactual peaks in the *RSF* at distances of less than  $\sim 1.5$  Å result from the Victoreen background<sup>23</sup> fit generally applied to the data and the imperfect background subtraction that results.) The peak positions in the *RSF* are shifted slightly from the true shell distances because of the phase shift  $\phi_j$  experienced by the photoelectrons in backscattering.

The e.x.a.f.s. data are analysed with single-electron single-scattering theory<sup>21</sup>:

$$\chi(k) = \sum \frac{N_j f_j(k)}{k R_j^2} \sin[2kR_j + \phi_j(k)] \exp(-2k_j^2 \sigma_j^2) \quad (1)$$

where the wavevector  $k$  is defined as follows:

$$k = (2\pi/h)[2m(E - E_0)]^{1/2} \quad (2)$$

with  $E$  being the incident X-ray energy,  $h$  is Planck's constant and  $m$  is the mass of an electron.  $E_0$  is approximately equal to the edge energy but is allowed to vary slightly to provide the best fit to the data and to correct for any errors in energy calibration<sup>24</sup>.  $\gamma_j$  accounts for the amplitude reduction due to inelastic scattering and is approximated by  $\exp(-2k_j/\lambda_j)$ , with  $\lambda_j$  defining a mean-free-path parameter for shell  $j$ . The  $\lambda_j$  are determined from model compounds as similar as possible to the system under investigation. (Metal oxides were used here as model compounds as they have metal-oxygen pairs in the first coordination shell and metal-metal pairs in the second shell, as found in the ionomer data presented here.) The functions  $f_j(k)$  and

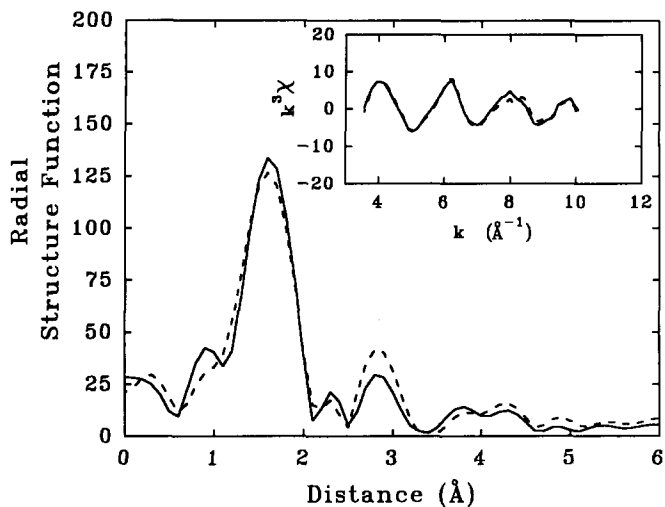


Figure 1 E.x.a.f.s. data for solvent-cast P1SNi (----) and E1SNi (—)

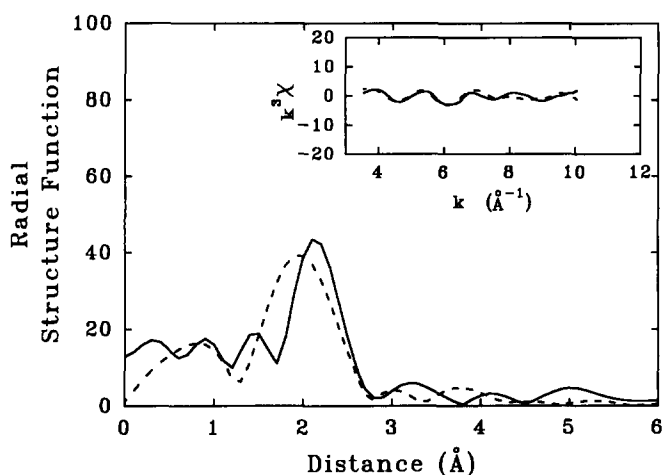


Figure 2 E.x.a.f.s. data for solvent-cast P1SSr (—) and E1SSr (----)

$\phi_j(k)$  are the backscattering amplitudes and phase-shift functions, respectively, which are characteristic of the types of atom in shell  $j$  and the absorbing atom. The theoretical calculations of Teo and Lee<sup>24</sup>, with slight modifications to accommodate experimental data from model compounds<sup>25</sup>, were utilized. To correct for minor errors in calculated phase shifts, differences between the  $R_j$  values determined by crystallography and e.x.a.f.s. were added to the  $R_j$  values found for the ionomers. The accuracies of  $R_j$  and  $N_j$  have been quoted as 1% and 20%, respectively<sup>26,27</sup>; however, these values depend strongly on the quality of the data. The signal-to-noise ratio and the breadth of the usable wavevector range influence the accuracy of  $R_j$  and  $N_j$ .

The e.x.a.f.s. data are presented in two forms. The first is a plot of  $k^3 \chi$  versus  $k$ , where the  $k^3$  factor is included to cancel approximately the diminishing wave amplitude at high  $k$  and allow a more uniform weighting in the regression fitting. The  $k^3 \chi$  data are Fourier transformed to yield the second plot, the *RSF*. In order to extract the structural parameters from the data, the contribution of each shell to the  $k^3 \chi$  spectrum is obtained by Fourier filtering. The Fourier transform is multiplied by a window function to isolate the peak of interest, and the result is inverse transformed to isolate the single-shell  $k^3 \chi$ . The chemical composition and structural parameters  $N_j, R_j$

and  $\sigma_j$  are postulated for the shell, and a model spectrum is calculated. The parameters are refined by non-linear regression. The quality of the fit is measured by  $Q$ , the square root of the ratio of the sum of the squares of the residue to the sum of the squares of the data. Finally, the calculated *RSF* is compared with that generated directly from the experimental data to check the validity of the modelling parameters.

The influence of cation type on the cation local environment can be clearly seen in the *RSF* and  $k^3 \chi$  plots for the P1S and E1S ionomers in Figures 1–3. Note the difference in scales between the figures. For the  $\text{Ni}^{2+}$ -neutralized ionomers, a strong first-shell coordination peak at 1.6 Å and a second-shell peak at 2.8 Å can be discerned in Figure 1. The *RSFs* of the  $\text{Sr}^{2+}$  ionomers, shown in Figure 2, display strong first-shell peaks and perhaps weak second-shell peaks. The *RSFs* of the  $\text{Cd}^{2+}$  ionomers of Figure 3 show a weak shell near 1.6 Å; the small peak height in the *RSF* indicates that the local structure is extremely disordered. The extent of local ordering observed in the *RSFs*, decreasing from  $\text{Ni}^{2+}$  to  $\text{Sr}^{2+}$  to  $\text{Cd}^{2+}$ , matches the physical property trends discussed in the accompanying paper<sup>1</sup>, as was seen previously with the sulphonated PTMO(1000)-based polyurethane ionomers<sup>3</sup> and the carboxy telechelic polyisoprenes<sup>2</sup>.

The results were quantified by fitting the first-shell peaks of the  $\text{Ni}^{2+}$  and  $\text{Sr}^{2+}$  ionomers and the second-shell peaks of the  $\text{Ni}^{2+}$  ionomers to equation (1). The parameters of the model compounds appear in Table 1; they were used to obtain the results for the ionomers listed in Table 2. The small size of the second-shell peak in the  $\text{Ni}^{2+}$  ionomers makes fitting the peak difficult, as shown by the anomalously high  $\sigma_2$  values; the smaller peaks are more distorted by

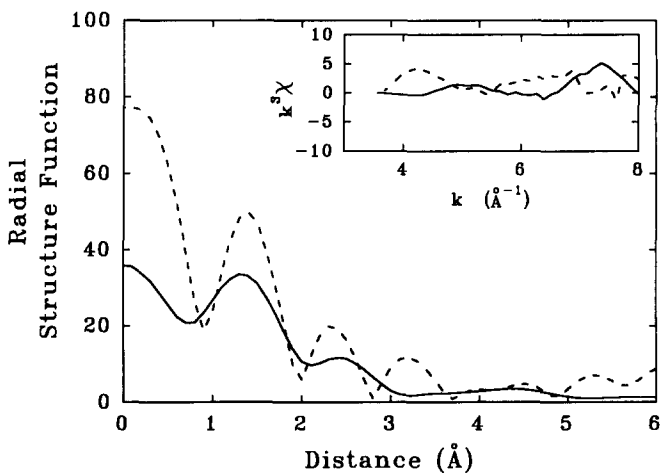


Figure 3 E.x.a.f.s. data for solvent-cast P1SCd (—) and compression-moulded E1SCd (----)

Table 1 Model compound parameters<sup>a</sup>

Compound	Shell number ( $j$ )	Shell element	$R_j$ (Å)	$N_j \rho_j$	$N_j$	$\lambda_j$ (Å)
NiO	1	O	2.09	2.47	6	4.59
	2	Ni	2.95	5.95	12	8.36
SrO	1	O	2.54	2.86	6	6.90

<sup>a</sup>Distance values and coordination numbers determined from crystallography

Table 2 E.x.a.f.s. structural parameters for dry ionomers

Sample	Sample preparation <sup>b</sup>	Shell number ( <i>j</i> )	Shell element	<i>R<sub>j</sub></i> (Å)	<i>N<sub>j</sub></i> / <i>j</i>	<i>N<sub>j</sub></i>	<i>σ<sub>j</sub></i> (Å)	<i>Q</i> (%)
M1CNi	SC	1	O	2.07	2.79	6.9	0.057	2.21
		2	Ni	3.07	2.28		0.132	4.82
M1SNi <sup>a</sup>	SC	1	O	2.08	3.36	8.3	0.075	1.83
		2	Ni	3.06	5.47		0.169	4.48
M2SNi	CM	1	O	2.09	3.09	7.7	0.044	3.83
		2	Ni	3.03	4.22		0.149	4.16
M2SSr	CM	1	O	2.52	1.96	4.1	0.064	7.40
M2CNi	CM	1	O	2.10	3.27	8.1	0.079	10.06
		2	Ni	3.07	1.73		0.116	9.38
M2CNi	SC	1	O	2.30	4.15	11.3	0.066	4.01
		2	Ni	3.27	1.53		0.110	4.51
P1SNi	SC	1	O	2.08	3.79	9.4	0.088	0.91
		2	Ni	3.13	1.60		0.111	1.13
P1SSr	SC	1	O	2.59	1.78	3.8	0.075	1.63
P2SNi	CM	1	O	2.09	3.33	8.3	0.071	1.72
		2	Ni	3.16	1.43		0.112	2.31
P2SNi	SC	1	O	2.10	3.49	8.7	0.071	4.68
		2	Ni	3.14	3.13		0.147	7.43
P2SSr	CM	1	O	2.60	1.81	3.8	0.089	8.72
P2SSr	SC	1	O	2.53	1.88	3.9	0.063	8.04
P2CNi <sup>c</sup>	CM	1	O	2.08	3.32	8.2	0.091	3.27
		2	Ni	3.10	0.49		0.051	3.01
P2CSr <sup>c</sup>	CM	1	O	2.50	2.06	4.3	0.076	10.74
E1SNi	SC	1	O	2.09	3.25	8.1	0.071	0.95
		2	Ni	3.14	2.01		0.144	0.80
E1SSr	SC	1	O	2.51	1.61	3.3	0.050	5.24

<sup>a</sup>From ref. 5<sup>b</sup>SC = solvent-cast, CM = compression-moulded<sup>c</sup>Neutralized to 100% excess of stoichiometric

background noise so that accurate second-shell coordination numbers could not be determined. The high degree of disorder in the Cd<sup>2+</sup> ionomers prevented extraction of satisfactory model parameters for these ionomers.

For all the ionomers studied in this paper, the first coordination shell was composed of oxygen atoms. Either water or the pendant anion could have contributed these oxygen atoms; however, complete coordination by the pendant anion is ruled out by the absence of a distinct coordination shell due to sulphur (for sulphonated ionomers) or carbon (for carboxylated ionomers). A cation structure completely coordinated to the pendant anion was observed previously for dehydrated zinc-neutralized sulphonated polystyrene ionomers<sup>10</sup>. The presence of water in the ionomers was expected because of the difficulty in completely drying polyurethane ionomers, as discussed previously<sup>3</sup>.

The coordination number *N<sub>j</sub>* for most of the Ni<sup>2+</sup> ionomers is within 20% of 6, the coordination number of the NiO model compound. Slightly higher values were found for some of the Ni<sup>2+</sup> ionomers; however, the samples with larger *N<sub>j</sub>* values also have larger Debye–Waller factors *σ<sub>j</sub>*. As equation (1) shows, *N<sub>j</sub>* is correlated to *σ<sub>j</sub>* so that ionomers with larger *σ<sub>j</sub>* would be likely to exhibit larger *N<sub>j</sub>*. Because of the similarity of the first-shell distance of the Ni<sup>2+</sup> ionomers to the model compound, it is likely that the first-shell coordination number of the Ni<sup>2+</sup> ionomers is 6. In contrast, the first-shell coordination number for the Sr<sup>2+</sup> ionomers appears to be in the range of 3–5, with the uncertainty arising from the inaccuracy inherent in determining *N<sub>j</sub>* from e.x.a.f.s. data.

#### Effect of polyol type and polyol molecular weight

Figure 1 compares similar sulphonated polyurethane ionomers based on PPO(1000) and PEO(1000) polyols. The change in polyol type has no effect on shell distances or coordination numbers for the Ni<sup>2+</sup> ionomers. A similar comparison for the Sr<sup>2+</sup> ionomers, shown in Figure 2, exhibits a slight shifting of the first-shell peak, which is reflected in the larger *R<sub>1</sub>* value for P1SSr (2.59 Å) than E1SSr (2.51 Å). Given the low peak heights for the Sr<sup>2+</sup> ionomers and, therefore, the lower signal-to-noise ratios, these differences are probably not significant. For P1SCd and E1SCd, the *RSFs* shown in Figure 3 do not agree completely, but again the disagreement may arise from the lower signal-to-noise ratio or the more limited wavevector range of the data. Since both ionomers display a locally disordered structure, it is likely that polyol type has little effect on local structure.

The cation environment is also nearly independent of polyol molecular weight or the ionic content of the polymers. Figure 4 shows the data for P2SNi. The solvent-cast P2SNi ionomer gives structural parameters that are indistinguishable from those of P1SNi, indicating that polyol molecular weight does not influence the local environment. Data for P2SSr, shown in Figure 5, yield *R<sub>1</sub>* and *N<sub>1</sub>* values that are essentially indistinguishable from those of P1SSr, given the quality of the data. Similarly, the *RSF* for P2SCd, shown in Figure 6, approximately matches that of P1SCd.

Polyol type also has no significant influence on the local cation environment for ionomers based on polyols of molecular weight 2000. M2SCd gives a slightly shifted first-shell peak compared with P2SCd, but the *RSF* of

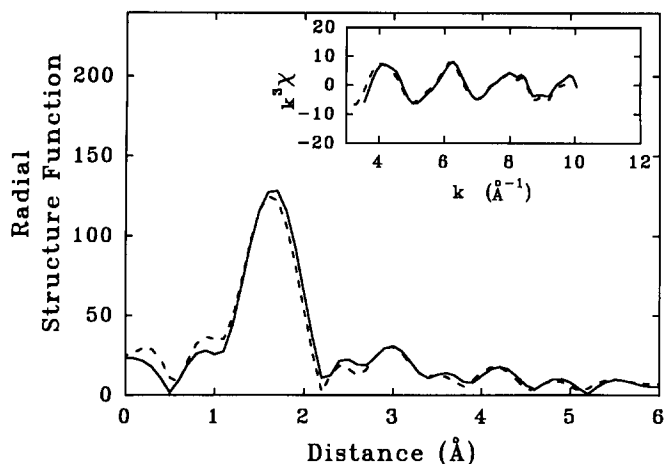


Figure 4 E.x.a.f.s. data for solvent-cast (—) and compression-moulded (----) P2SNi

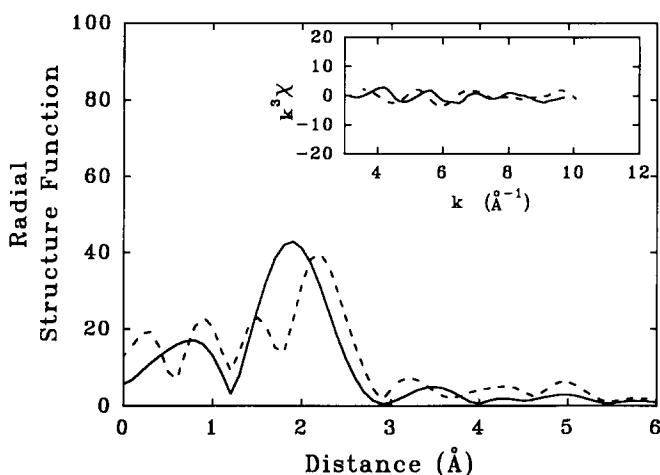


Figure 5 E.x.a.f.s. data for solvent-cast (—) and compression-moulded (----) P2SSr

M2SCd is essentially identical to that of P2SCd within experimental accuracy. The data for M2SSr, shown in Figure 7, give approximately the same  $R_1$  and  $N_1$  values as are obtained for the solvent-cast P2SSr ionomer.

*Effect of anion type*

Pendant anion type has only a small influence on the local environment of the neutralizing cation. The RSF for M1CNi, shown in Figure 8, shows two coordination shells, as was previously seen for an M1SNi ionomer<sup>5</sup>. Comparing the structural parameters for M1CNi and M1SNi<sup>5</sup>, the coordination shell distances are identical, but the Debye-Waller factors are somewhat less for the M1CNi ionomer. As was discussed in the previous paper<sup>1</sup>, there is only one coordination edge of the carboxylate anion available for interaction with the cation, whereas there are two possible coordination positions in the sulphonated ionomer, depending upon whether the cation coordinates to the edge or to the face of the sulphonate tetrahedron. Assuming equivalent degrees of hydration in M1SNi and M1CNi, the differences in the  $\sigma_j$  values could reflect the greater disorder in the sulphonate aggregates introduced by having two coordination positions.

A comparison can also be made of the data for compression-moulded M2CNi, shown in Figure 8, and

compression-moulded M2SNi, shown in Table 2. The coordination distances and numbers essentially match for the first-shell peak, but  $R_2$  and  $\sigma_2$  are slightly less for M2CNi than for M2SNi. Once again, this could reflect differences resulting from anion geometry.

Finally, comparing data for the PTMO-based, Cd<sup>2+</sup>-neutralized ionomers, shown in Figures 6 and 9, a slight shifting of the peak between the sulphonated and carboxylated ionomers is observed, but the same generally disordered local structure is maintained. Thus, while anion type has a small influence on the ordering in the immediate vicinity of the cation, the effect is small compared with the impact of the neutralizing cation itself.

*Effect of overneutralization*

In a previous study of telechelic sulphonated polyisobutylene ionomers neutralized with zinc<sup>13</sup>, Vlaic *et al.* showed that the presence of a 10% or 100% stoichiometric excess of neutralizing cation had no effect on the cation local environment. Figure 10 shows the RSFs for the two polyurethane ionomers that were neutralized with 100% excess of neutralizing cation. Comparing the  $R_j$  and  $N_j$  values with those for ionomers neutralized with an exact stoichiometric amount of cation, it is seen that the structural parameters and the local environment are unchanged by the presence of excess cation.

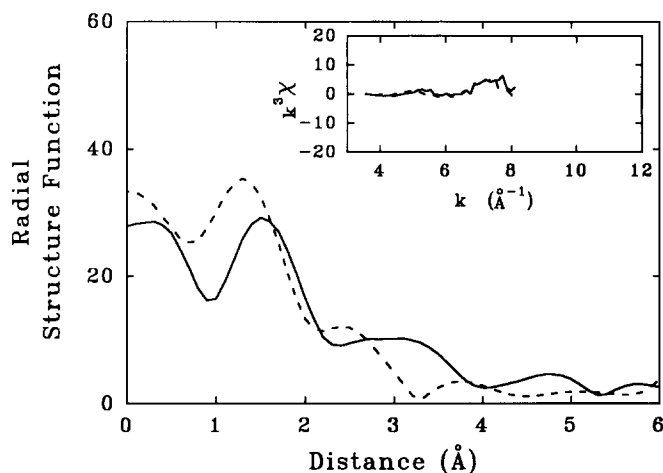


Figure 6 E.x.a.f.s. data for compression-moulded P2SCd (—) and M2SCd (----)

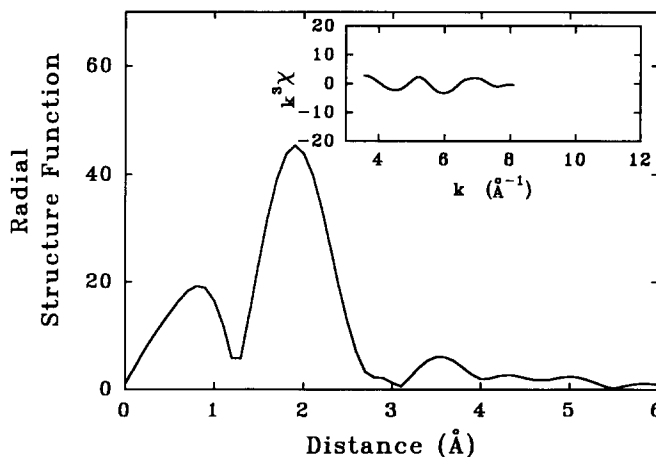


Figure 7 E.x.a.f.s. data for compression-moulded M2SSr

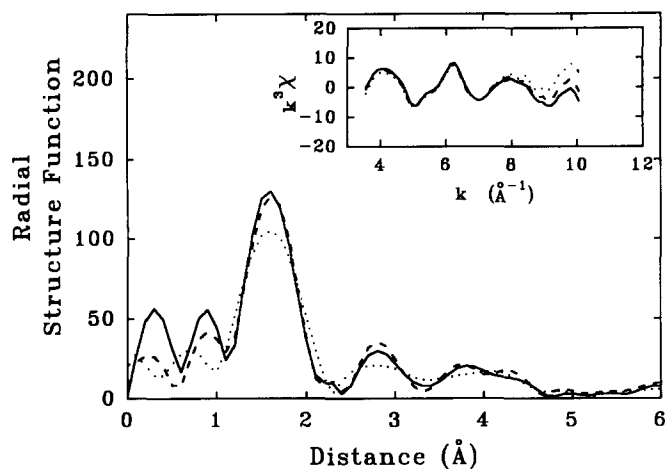


Figure 8 E.x.a.f.s. data for solvent-cast M1CNi (—) and M2CNi (---) and for compression-moulded M2CNi (.....)

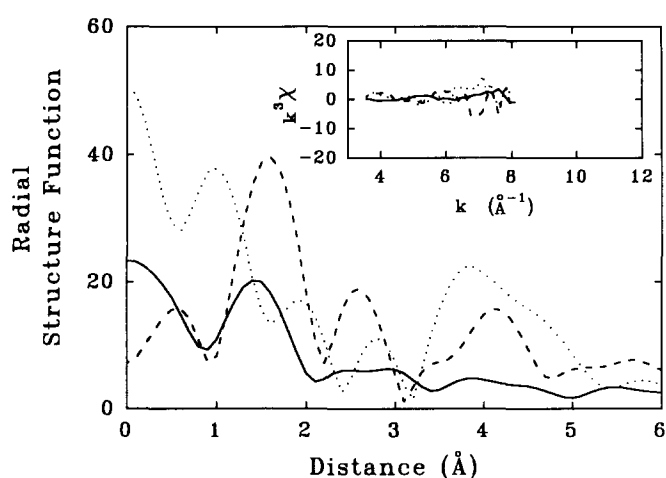


Figure 9 E.x.a.f.s. data for solvent-cast M1CCd (—) and M1SCd (---) and for compression-moulded M2CCd (.....)

#### Effect of sample preparation conditions

Many sample preparation conditions result in the establishment of non-equilibrium structure in polymers. Thus, sample preparation conditions have a strong influence on polymer properties. Sample preparation conditions were studied for three ionomers, P2SNi (Figure 4), P2SSr (Figure 5) and M2CNi (Figure 8). For the P2SNi ionomer, no change in the cation local environment was observed between the compression-moulded and solvent-cast samples; the  $R_j$  and  $N_j$  values remained essentially constant. The slight difference in the  $R_1$  values for the compression-moulded and solvent-cast P2SSr ionomers is also within the accuracy limits of the experiment. In contrast, the solvent-cast and compression-moulded M2CNi ionomers display shifts in the first- and second-shell coordination peaks, which are reflected in the  $R_j$  values. The  $R_1$  and  $R_2$  values of the solvent-cast M2CNi ionomer are 0.2 Å greater than those of the compression-moulded ionomer, and the first-shell coordination number is greater for the solvent-cast ionomer. These changes in local environment probably reflect the presence of residual methanol in the ionic aggregates of the solvent-cast ionomer, giving rise to a slightly more disordered structure than in the compression-moulded sample. A greater degree of disorder in the solvent-cast sample is also reflected in its lower first-shell peak height in the RSF.

#### Effect of hydration

Compression-moulded discs of a carboxylated and a sulphonated polyurethane ionomer were immersed in water for varying periods of time to study the effect of hydration time on the cation environment. The RSFs for M2SNi appear in Figure 11; for times greater than zero, the RSFs are arbitrarily offset for clarity. The structural parameters extracted from these data appear in Table 3. While the sulphonated sample was visibly observed to change from translucent to opaque as hydration proceeded, the first-shell coordination number remained constant, and the Ni–O distance remained unchanged at 2.1 Å after 70 min of hydration. The second-shell coordination distance also remained unchanged, as did the second-shell peak height. This contrasts with previously published data for dry and hydrated (30 min)

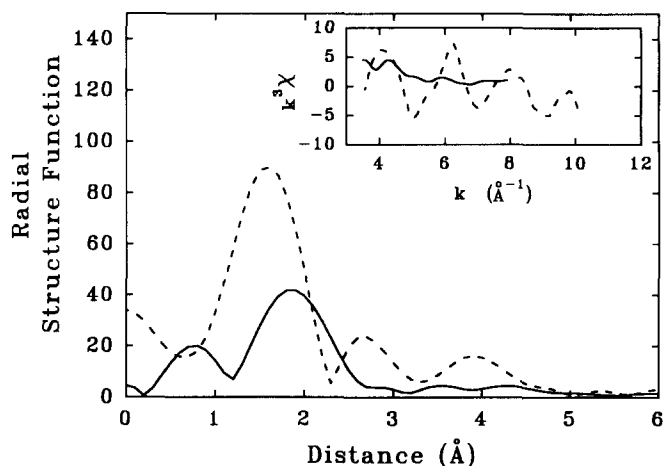


Figure 10 E.x.a.f.s. data for ionomers neutralized with 100% stoichiometric excess: P2CSr (—); P2CNi (---)

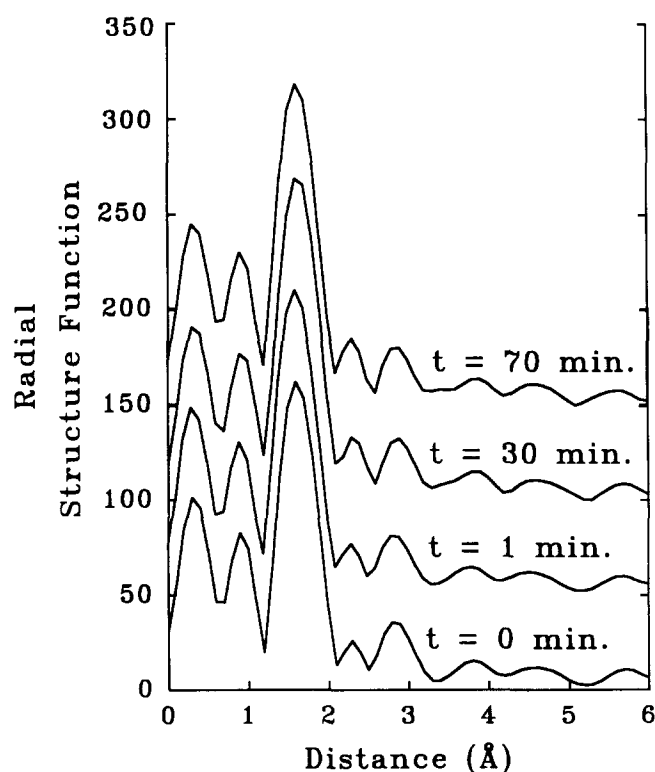
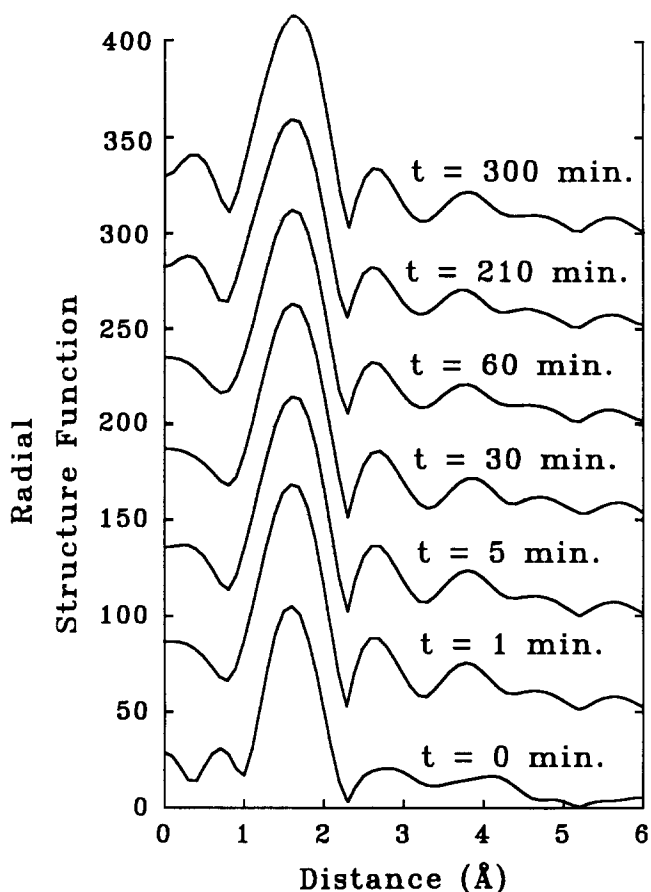


Figure 11 E.x.a.f.s. hydration data for M2SNi. Curves for times greater than zero are arbitrarily offset for clarity

**Table 3** E.x.a.f.s. parameters for hydrated M2SNi

Hydration time (min)	Shell number ( <i>j</i> )	Shell element	$R_j$ (Å)	$N_{j j}$	$N_j$	$\sigma_j$ (Å)	$Q$ (%)
0	1	O	2.09	3.09	7.7	0.044	3.83
	2	Ni	3.03	4.22		0.149	4.16
1	1	O	2.09	3.07	7.6	0.045	3.65
	2	Ni	3.05	3.19		0.146	3.93
30	1	O	2.09	3.58	8.9	0.055	3.74
	2	Ni	3.05	3.50		0.143	2.49
70	1	O	2.08	3.23	8.0	0.044	3.74
	2	Ni	3.04	2.55		0.133	2.51

**Figure 12** E.x.a.f.s. hydration data for M2CNi. Curves for times greater than zero are arbitrarily offset for clarity**Table 4** E.x.a.f.s. parameters for hydrated M2CNi

Hydration time (min)	Shell number ( <i>j</i> )	Shell element	$R_j$ (Å)	$N_{j j}$	$N_j$	$\sigma_j$ (Å)	$Q$ (%)
0	1	O	2.10	3.27	8.1	0.079	10.06
	2	Ni	3.07	1.73		0.116	9.38
1	1	O	2.06	5.00	12.3	0.110	3.56
	2	Ni	3.05	4.26		0.154	1.75
5	1	O	2.07	4.96	12.2	0.111	3.84
	2	Ni	3.05	3.13		0.143	1.68
30	1	O	2.06	4.80	11.8	0.109	3.89
	2	Ni	3.06	2.14		0.126	1.82
60	1	O	2.07	4.60	11.4	0.106	4.59
	2	Ni	3.06	1.49		0.113	2.66
210	1	O	2.07	4.77	11.8	0.110	5.58
	2	Ni	3.06	0.81		0.078	4.11
300	1	O	2.07	5.08	12.5	0.112	4.86
	2	Ni	3.06	0.73		0.066	3.24

solvent-cast M1SNi, where the height of the second-shell peak increased markedly upon hydration<sup>5</sup>. Differences probably arise from transport limitations. M2SNi is an ~1 mm thick disc; the M1SNi stacked films were ~0.2 mm thick each. As the non-polar polymer matrix would serve as a barrier to diffusion of water to the ionic aggregates, the persistence of local order in M2SNi upon hydration probably indicates that the water could not diffuse completely to the ionic aggregates; the sample did not reach equilibrium levels of hydration. The visible change of the sample from dark green to a whitish green indicates that water is permeating the sample, however.

The *RSF* data for M2CNi at various hydration times appear in *Figure 12* and *Table 4*. Like the sulphonated ionomer, the Ni–O first-shell distance in the carboxylated ionomer remains constant at 2.1 Å; however, the carboxylated ionomer exhibits a sharp increase in first-shell coordination number after only 1 min immersion in water. The larger ionic aggregate size seen in carboxylated ionomers compared with sulphonated ionomers<sup>28</sup> may allow water to diffuse into the ionic regions more quickly, enabling the water to coordinate to the cation. Alternatively, water diffusion in the carboxylated ionomer could be facilitated by a greater number of ionic groups dispersed in the polymer matrix or a less densely packed polymer matrix. The presence of crystallites in M2CNi<sup>1</sup> lends some credence to the latter explanation. Unfortunately, because  $\sigma_1$  increases along with  $N_1$  as hydration time progresses, no definitive conclusions regarding changes in first-shell coordination can be drawn. In contrast to the first shell, the disorder  $\sigma_2$  in the second shell decreases after the 60 min time point. This may simply reflect a decrease in the number of coordinating metal atoms in the second shell; however, it indicates that a hydration time of greater than 60 min, and probably greater than 70 min if the M2SNi data are considered, is required for these ionomers before changes in the local environment are observed. The changes in coordination number are consistent with the observed influence of water on the physical properties of ionomers.

## CONCLUSIONS

The variety of model polyurethane ionomers studied by e.x.a.f.s. demonstrates that local ordering is primarily determined by the nature of the neutralizing cation. Polyol type and molecular weight, pendant anion type,

the presence of excess neutralizing agent, and some sample preparation conditions were shown to have at most a slight effect on the local environment. For one sample, M2CNI, preparation conditions had a strong effect, illustrating the importance of this consideration. The otherwise small effect on the local environment of these factors, however, does not imply that the structure within the ionic aggregates remains constant with the changing conditions. E.x.a.f.s. probes only the local environment of each cation; it does not generally provide crystallographic data, nor does it accurately count chemical species. Thus, changes in aggregate structure on a size scale of greater than  $\sim 5 \text{ \AA}$  would not be detected by e.x.a.f.s. Also, e.x.a.f.s. probes only the average cation environment. It has been assumed that cations residing in the aggregates form more locally ordered structures and, therefore, that they represent the primary contribution to the e.x.a.f.s. results. However, it is also possible that cations dispersed in the matrix provide contributions to the e.x.a.f.s. data that distort the data's relevance to the pure aggregate structure. Differences in local structure within each ionomer may be masked by the inherent averaging of the e.x.a.f.s. technique. The e.x.a.f.s. data do not exclude the probability of different packing arrangements in the ionic aggregates of carboxylated and sulphonated ionomers or of polyurethane ionomers based on different polyol types.

The first coordination shell in all the ionomers examined arose from oxygen. As no second-shell sulphur or carbon peaks could be discerned, complete coordination by the pendant anion is not occurring; water molecules absorbed during handling also contribute to the first shell. Direct evidence for water coordination could not be obtained, as hydrogen atoms are poor electron scatterers and are not visible by e.x.a.f.s. However, the hydration experiments showed an increase in first-shell coordination number after sufficient hydration time had elapsed for water diffusion to the cations, but the hydrated ionomers showed no change in first-shell coordination distances. If sulphonate or carboxylate oxygen atoms were exclusively responsible for the first shell, a change in first-shell coordination distance with hydration would be expected as water molecules displaced the anions. While many of the first-shell oxygen atoms arise from the pendant anion, such species are only one component.

While the  $\text{Cd}^{2+}$  cation displayed only a disordered first shell,  $\text{Sr}^{2+}$  showed a well defined first shell, and  $\text{Ni}^{2+}$  had definite first and second shells. The second shell was attributed to metal atoms, and the metal-metal distances observed are consistent with those observed by e.x.a.f.s. in nickel-neutralized<sup>15</sup> and iron-neutralized<sup>16</sup> Nafions and in nickel- and zinc-neutralized carboxy-telechelic polyisoprenes<sup>2</sup>. The presence of such a well defined metal-metal distance indicates that the two metal atoms are somehow connected, such as by bridging through hydroxyl groups<sup>16</sup>, where two metal atoms share oxygen atoms in their first coordination shells. The nature of the bridging oxygen is difficult to discern by e.x.a.f.s., however. Nevertheless, the existence of such bridged structures implies the formation of more cohesive aggregates, as removal of an ionic group from an

aggregate would require disruption of the bridge structure. Not surprisingly, then, the degree of local order decreases from  $\text{Ni}^{2+}$  to  $\text{Sr}^{2+}$  to  $\text{Cd}^{2+}$ , as do the tensile properties of the polyurethane ionomers<sup>1</sup>.

## ACKNOWLEDGEMENTS

Support for this work was provided by US Department of Energy through Grant DE-FG02-88ER45370; by the donors of the Petroleum Research Fund, administered by the American Chemical Society, through Grant 20343-AC7; and by Fellowships for S.A.V. from the National Science Foundation and the Wisconsin Alumni Research Foundation. Special thanks are due to Brian P. Grady for his help in collecting the e.x.a.f.s. data presented in this work.

## REFERENCES

- 1 Visser, S. A. and Cooper, S. L. *Polymer* 1992, **33**, 920
- 2 Register, R. A., Foucart, M., Jerome, R., Ding, Y. S. and Cooper, S. L. *Macromolecules* 1988, **21**, 2652
- 3 Ding, Y. S., Register, R. A., Yang, C.-Z. and Cooper, S. L. *Polymer* 1989, **30**, 1204
- 4 Ding, Y. S., Register, R. A., Yang, C.-Z. and Cooper, S. L. *Polymer* 1989, **30**, 1213
- 5 Ding, Y. S., Register, R. A., Yang, C.-Z. and Cooper, S. L. *Polymer* 1989, **30**, 1221
- 6 Ward, T. C. and Tobolsky, A. V. *J. Appl. Polym. Sci.* 1967, **11**, 2903
- 7 Sakamoto, K., MacKnight, W. J. and Porter, R. S. *J. Polym. Sci. (A-2)* 1970, **8**, 277
- 8 Hara, M., Eisenberg, A., Storey, R. F. and Kennedy, J. P. in 'Coulombic Interactions in Macromolecular Systems', (Eds. A. Eisenberg and F. E. Bailey), ACS Symp. Ser. 302, American Chemical Society, Washington, DC, 1986
- 9 Yarusso, D. J., Ding, Y. S., Pan, H. K. and Cooper, S. L. *J. Polym. Sci., Polym. Phys. Edn.* 1984, **22**, 2073
- 10 Ding, Y. S., Yarusso, D. J., Pan, H. K. and Cooper, S. L. *J. Appl. Phys.* 1984, **56**, 2396
- 11 Ding, Y. S., Register, R. A., Nagarajan, M. R., Pan, H. K. and Cooper, S. L. *J. Polym. Sci., Polym. Phys. Edn.* 1988, **26**, 289
- 12 Register, R. A., Weiss, R. A., Li, C. and Cooper, S. L. *J. Polym. Sci., Polym. Phys. Edn.* 1989, **27**, 1911
- 13 Vlais, G., Williams, C. E., Jerome, R., Tant, M. R. and Wilkes, G. L. *Polymer* 1988, **29**, 173
- 14 Vlais, G., Williams, C. E. and Jerome, R. *Polymer* 1987, **28**, 1566
- 15 Pan, H. K., Yarusso, D. J., Knapp, G. S. and Cooper, S. L. *J. Polym. Sci., Polym. Phys. Edn.* 1983, **21**, 1389
- 16 Pan, H. K., Yarusso, D. J., Knapp, G. S., Pineri, M., Meagher, A., Coey, J. M. D. and Cooper, S. L. *J. Chem. Phys.* 1983, **79**, 4736
- 17 Pan, H. K., Meagher, A., Pineri, M., Knapp, G. S. and Cooper, S. L. *J. Chem. Phys.* 1985, **82**, 1529
- 18 Pan, H. K., Knapp, G. S. and Cooper, S. L. *Colloid Polym. Sci.* 1984, **262**, 734
- 19 Visser, S. A. and Cooper, S. L. *Macromolecules* 1991, **24**, 2576
- 20 Sayers, D. E., Stern, E. A. and Lytle, F. W. *Phys. Rev. Lett.* 1971, **27**, 1024
- 21 Stern, E. A., Sayers, D. E. and Lytle, F. W. *Phys. Rev. (B)* 1975, **11**, 4836
- 22 Lee, P. A., Citrin, P. H., Eisenberger, P. and Kincaid, B. M. *Rev. Mod. Phys.* 1981, **53**, 769
- 23 Victoreen, J. A. *J. Appl. Phys.* 1948, **19**, 855
- 24 Teo, B. K. and Lee, P. A. *J. Am. Chem. Soc.* 1979, **101**, 2815
- 25 Pan, H. K. Ph.D. Thesis, University of Wisconsin-Madison, 1983
- 26 Lengler, B. and Eisenberg, P. *Phys. Rev. (B)* 1980, **22**, 4507
- 27 Stern, E. A. and Kim, K. *Phys. Rev. (B)* 1981, **23**, 781
- 28 Visser, S. A. and Cooper, S. L. *Macromolecules* 1991, **24**, 2584